Supporting Information for "Rupture Termination in Laboratory-Generated Earthquakes"

Chun-Yu Ke[1], Gregory C. McLaskey[1], and David S. Kammer[1]

[1]School of Civil and Environmental Engineering, Cornell University, Ithaca, New York, USA

Contents of this file

1. Text S1
2. Figures S1 to S2
3. Tables S1

Introduction

The data used are continuous fault slip and strain data collected from a set of laboratory biaxially loaded direct shear experiments with a pair of 3 m long granite samples. The continuous data was then separated in time with one-second window centering the timings of dynamic slip events. Spatial representations of slip data was linearly interpolated across the length of the 3 m fault using 16 evenly spaced measurements; strain and stress was interpolated with cubic Hermite spline (pchip) from 8 locations to obtain smooth continuous functions of space. Imperfections in experiments are listed in Table S1.

Text S1. Solving rupture termination for bilateral confined slip events

For bilateral confined slip events, we chose the maximum of $\tau_0(x)/\sigma_0(x)$ as an initial prescribed location of x_c, and gradually increased a to compute values of $K^s_{\mathrm{II}}(x)$ at $x = x_c \pm a$. The position of $G^s_{\mathrm{II}}(x) = \mathit{\Gamma}(x)$ is different for both crack tips due to the slightly non-symmetric stress state. Therefore, we first find the shorter crack half-length a, fix it, and then extend the crack unilaterally in the opposite direction to find the second arrest position, while x_c is updated accordingly. This approach yields G^s_{II} at the first fixed end slightly higher than $\mathit{\Gamma}$ since the extension of a on the other end also increases the value of G^s_{II} on the first fixed end. The estimation was refined by taking the center of the computed ruptured region as the updated x_c and restarting the computation recursively. The ruptured region converged within a few iterations with this operation.

Corresponding author: Gregory C. McLaskey, `gcm8@cornell.edu`

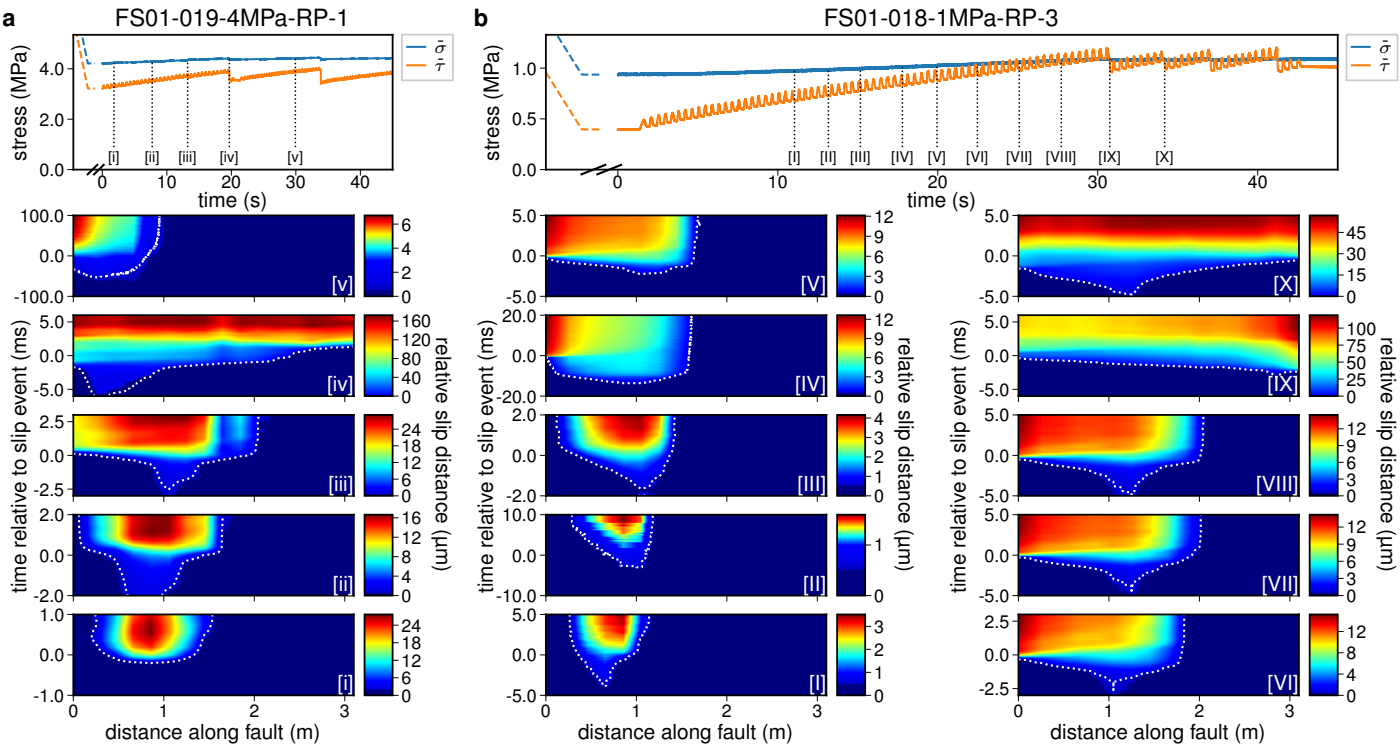

Figure S1. Sequences of laboratory earthquakes that occur after $\bar{\sigma}$ was decreased (a) from 7 MPa to 4 MPa and (b) from 4 MPa to 1 MPa. These events nucleate near $x \approx 1$ m and propagate bilaterally. The oscillation visible in $\bar{\tau}$ is due to the hydraulic pump.

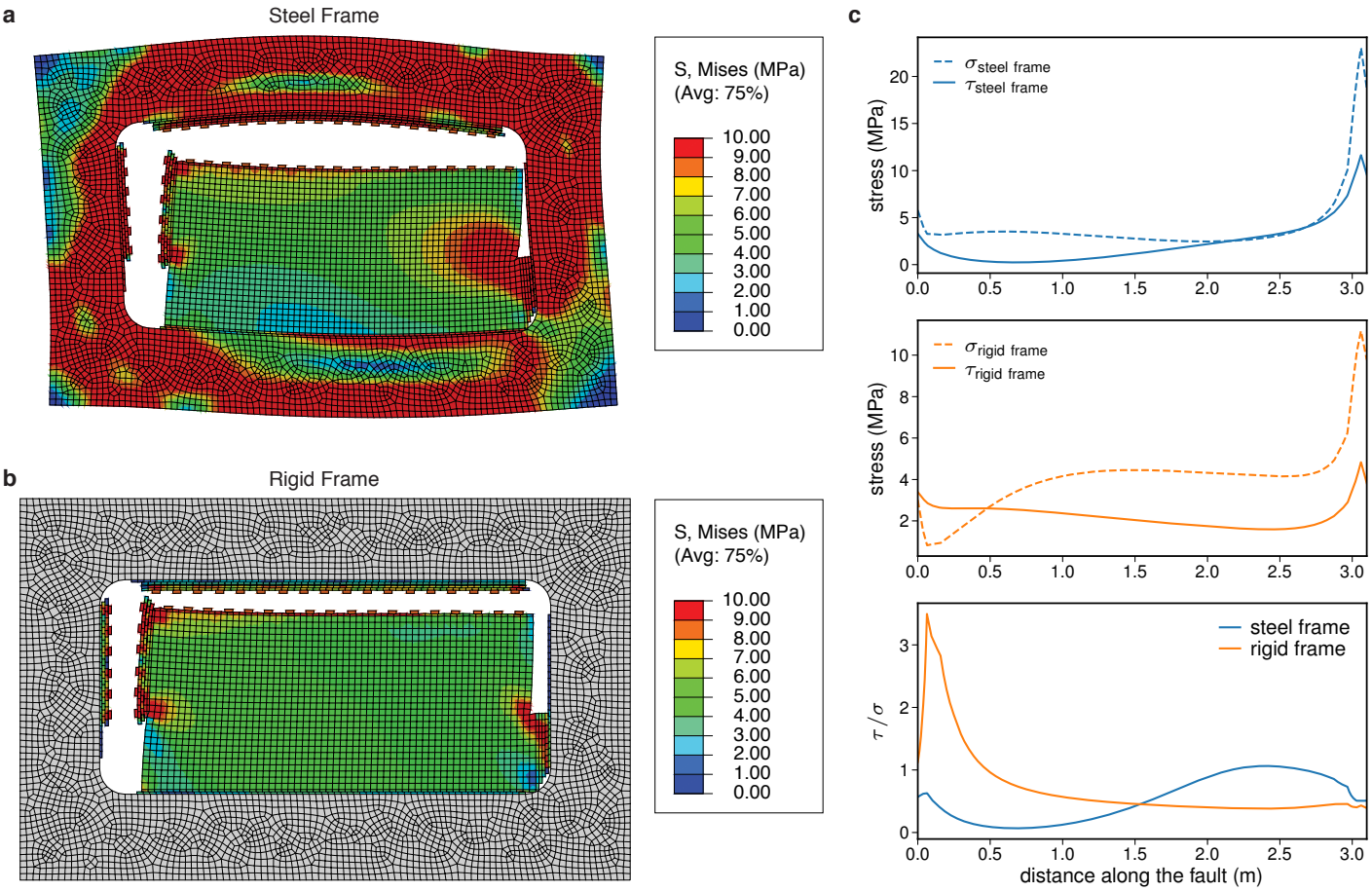

Figure S2. Finite element analysis with (a) elastic steel frame and (b) rigid frame. The simulated hydraulic loading was set to pressure levels measured before the first slip event of a sequence conducted at $\bar{\sigma} = 4$MPa, similar to the sequence shown in Figure 2b. The deformation is amplified by a factor of 200. **c**, Stress distribution along the fault. The stress ratio (τ/σ) of this apparatus (steel frame) is maximum at $x \approx 2$ m, which coincides with the point of nucleation for bilateral confined ruptures. Whereas the stress ratio peaks at $x \approx 0$ for a set-up with a rigid frame, which explains why experiments with compliant samples (Bayart et al., 2016; Maegawa et al., 2010; Rubinstein et al., 2007) always nucleate at the forcing end.

Table S1. Listing of Slip Events

Experiment FS01-	Event #	Time (sec)	$\bar{\sigma}$ (MPa)	$\bar{\tau}$ (MPa)	x_l (m)	x_r (m)	max. slip (µm)	Propagation	Confinement
013-4MPa-P-1	1	248.39	4.09	2.77	1.33	3.06	17.28	bilateral	full
	2	283.41	4.12	3.02	1.04	—	31.36	bilateral	partial[#]
	3	338.41	4.18	3.41	—	—	123.04	—	none
	4	387.38	4.20	3.58	—	—	267.04	—	none
	5	443.22	4.19	3.62	—	—	296.00	—	none
	6	487.58	4.16	3.53	—	—	214.24	—	none
	7	535.36	4.16	3.52	—	—	229.28	—	none
	8	588.18	4.16	3.53	—	—	241.11	—	none
	9	635.00	4.16	3.54	—	—	229.44	—	none
	10	686.13	4.16	3.52	—	—	231.68	—	none
015-4MPa-1*	1	36.57	4.12	2.59	1.42	2.88	13.44	bilateral	full
	2[‡]	61.25	4.16	2.85	1.23	3.05	19.04	bilateral	full
	3	95.74	4.21	3.16	0.94	—	46.88	bilateral	partial[#]
	4	132.30	4.28	3.54	—	—	140.00	—	none
	5	161.41	4.28	3.70	—	—	234.72	—	none
	6	187.76	4.27	3.62	—	—	172.32	—	none
	7	212.18	4.26	3.64	—	—	188.64	—	none
	8	251.37	4.28	3.68	—	—	220.81	—	none
	9	401.93	4.27	3.72	—	—	255.68	—	none
015-7MPa-P-1	1	154.34	7.13	5.28	—	—	85.28	—	none
	2	207.43	7.17	5.74	—	—	376.48	—	none
	3	242.03	7.07	5.45	—	1.20	34.40	unilateral	partial
	4	265.65	7.12	5.66	—	—	367.04	—	none
	5	303.40	7.06	5.41	—	1.25	28.00	unilateral	partial
	6	323.60	7.09	5.68	—	—	367.21	—	none
	7	366.19	7.06	5.48	—	1.39	38.55	unilateral	partial
	8	387.20	7.10	5.70	—	—	413.91	—	none
	9	432.61	7.04	5.39	—	1.47	36.63	unilateral	partial
	10	590.45	7.10	5.72	—	—	451.03	—	none
017-4MPa-P-1	1	177.97	4.22	3.30	1.20	2.72	14.40	bilateral	full
	2	237.57	4.30	3.66	—	—	161.44	—	none
	3	285.96	4.31	3.74	—	—	238.24	—	none
	4	334.09	4.32	3.74	—	—	228.80	—	none
	5	374.01	4.31	3.72	—	—	201.92	—	none
	6	578.07	4.34	3.81	—	—	273.45	—	none
017-4MPa-RP-1[§]	1	283.39	4.52	3.63	0.05	1.48	12.16	bilateral	full[¶]
	2	324.91	4.58	3.87	—	2.11	56.80	unilateral	partial
	3	378.11	4.68	4.15	—	—	342.24	—	none
	4	450.46	4.63	3.92	—	1.48	32.00	unilateral	partial
	5	505.63	4.71	4.20	—	—	417.60	—	none
017-7MPa-P-1	1	59.33	7.11	5.34	0.93	—	69.93	bilateral	partial[#]
	2	59.93	7.08	5.23	—	0.66	29.28	unilateral	partial
	3	95.62	7.11	5.54	—	0.90	30.72	unilateral	partial
	4	126.06	7.16	5.81	—	—	403.20	—	none
	5	206.77	7.11	5.76	—	—	404.97	—	none
	6	259.52	7.06	5.52	—	1.30	36.80	unilateral	partial
	7	299.18	7.12	5.86	—	—	450.56	—	none
018-1MPa-RP-3[§] [‖]	1	14.04	0.98	0.69	0.01	1.18	5.28	bilateral	full
	2	16.16	0.98	0.73	0.07	1.50	3.52	bilateral	full
	3	18.16	0.99	0.84	0.05	1.47	5.76	bilateral	full
	4	20.79	1.02	0.86	—	1.66	12.48	unilateral	partial
	5	22.95	1.02	0.89	—	1.67	12.80	unilateral	partial
	6	25.48	1.04	0.95	—	1.88	16.16	unilateral	partial
	7	28.10	1.06	0.99	—	2.00	14.88	unilateral	partial
	8	30.72	1.07	1.05	—	2.08	15.04	unilateral	partial
	9	33.75	1.10	1.09	—	—	117.44	—	none
	10	37.18	1.08	1.07	—	—	58.40	—	none
	11	40.05	1.09	1.09	—	—	77.12	—	none
	12	44.23	1.09	1.18	—	—	97.44	—	none
018-4MPa-P-2	1	42.40	4.14	2.99	1.35	3.07	15.52	bilateral	full
	2	53.58	4.19	3.27	0.95	—	39.36	bilateral	partial[#]
	3	69.70	4.24	3.63	—	—	198.56	—	none
	4	91.19	4.24	3.70	—	—	189.28	—	none

Continued on Next Page

Table S1. Listing of Slip Events – Continued from Previous Page

Experiment FS01-	Event #	Time (sec)	$\bar{\sigma}$ (MPa)	$\bar{\tau}$ (MPa)	x_l (m)	x_r (m)	max. slip (µm)	Propagation	Confinement
018-4MPa-P-3	1	102.44	4.16	3.13	1.26	—	16.96	bilateral	partial#
	2	127.47	4.22	3.43	0.82	—	58.08	bilateral	partial#
	3	146.76	4.24	3.65	—	—	159.68	—	none
	4	170.41	4.24	3.64	—	—	182.88	—	none
018-7MPa-P-1	1	22.14	6.92	4.01	1.85	2.65	4.00	bilateral	full
	2	37.93	6.99	4.45	1.42	2.88	16.80	bilateral	full
	3	59.91	7.09	4.97	1.22	—	47.52	bilateral	partial#
	4	88.52	7.19	5.71	—	—	208.96	—	none
	5	107.68	7.16	5.80	—	—	314.72	—	none
	6	126.74	7.12	5.68	—	—	167.36	—	none
	7	140.19	7.12	5.67	—	—	207.68	—	none
	8	154.93	7.11	5.63	—	—	187.20	—	none
	9	168.64	7.11	5.67	—	—	228.81	—	none
	10	181.98	7.12	5.66	—	—	198.41	—	none
019-4MPa-P-1	1	18.48	4.11	2.47	1.84	2.65	2.72	bilateral	full
	2	28.32	4.17	2.71	1.65	2.73	8.64	bilateral	full
	3	39.88	4.20	2.98	1.25	2.89	16.80	bilateral	full
	4	52.18	4.26	3.38	0.50	—	50.88	bilateral	partial#
	5	69.65	4.33	3.75	—	—	259.04	—	none
	6	84.60	4.28	3.67	—	—	174.40	—	none
	7	96.38	4.29	3.63	—	—	184.64	—	none
019-4MPa-RP-1	1	26.80	4.23	3.27	0.11	1.66	22.88	bilateral	full¶
	2	32.73	4.28	3.51	0.03	1.68	19.68	bilateral	full
	3	38.22	4.34	3.77	—	2.05	35.04	unilateral	partial
	4	44.68	4.41	3.93	—	—	172.00	—	none
	5	54.92	4.41	3.87	—	1.07	7.04	unilateral	partial
	6	58.87	4.44	3.97	—	—	268.48	—	none
	7	74.49	4.45	3.95	—	—	236.80	—	none
019-7MPa-P-1	1	20.32	7.03	4.16	1.76	2.65	7.36	bilateral	full
	2	33.83	7.12	4.65	1.62	2.88	21.92	bilateral	full
	3	53.64	7.22	5.29	1.21	—	68.64	bilateral	partial#
	4	60.67	7.22	5.38	—	0.46	12.48	unilateral	partial
	5	71.21	7.30	5.70	—	0.49	11.52	unilateral	partial
	6	76.29	7.31	5.91	—	1.11	30.88	unilateral	partial
	7	83.59	7.38	6.12	—	—	425.60	—	none
	8	105.98	7.28	5.80	—	—	38.72	—	none
	9	117.09	7.34	6.15	—	—	522.40	—	none
019-8MPa-1†	1	50.69	8.03	6.07	—	0.72	39.68	unilateral	partial
	2	70.78	8.08	6.41	—	1.55	48.96	unilateral	partial
	3	76.34	8.12	6.45	—	—	453.13	—	none
	4‡	109.68	8.00	6.25	—	1.74	48.79	unilateral	partial
	5	127.73	8.06	6.45	—	—	521.77	—	none
	6	154.75	7.95	6.05	—	0.90	32.79	unilateral	partial
020-4MPa-P-1	1	71.35	4.07	2.79	1.43	2.87	14.72	bilateral	full
	2	85.56	4.11	3.01	1.20	3.06	19.52	bilateral	full
	3	97.45	4.16	3.30	0.81	—	57.12	bilateral	partial#
	4	114.51	4.23	3.63	—	—	205.44	—	none
	5	126.66	4.21	3.64	—	—	176.16	—	none
	6	138.55	4.22	3.74	—	—	200.01	—	none
020-7MPa-RP-1	1	67.99	7.56	6.19	—	2.06	65.12	unilateral	partial
	2	83.70	7.68	6.57	—	—	376.48	—	none
	3	103.41	7.67	6.32	—	—	191.20	—	none
	4	126.65	7.72	6.51	—	—	329.60	—	none
	5	155.89	7.74	6.52	—	—	374.08	—	none

* Shown in Figure 2a.
† Shown in Figure 2b.
‡ Shown in Figure 3.
§ Shown in Figure S1.
‖ Discarded because the stress change was below the amplitude of error.
¶ Discarded because x_l is too close to $x = 0$, where strain was not measured.
\# Discarded because the partially confined bilateral rupture contradicts the assumption in theory.

References

Bayart, E., Svetlizky, I., & Fineberg, J. (2016). Fracture mechanics determine the lengths of interface ruptures that mediate frictional motion. *Nature Physics*, *12*(2), 166–170. doi: 10.1038/nphys3539

Maegawa, S., Suzuki, A., & Nakano, K. (2010). Precursors of global slip in a longitudinal line contact under non-uniform normal loading. *Tribology Letters*, *38*(3), 313–323. doi: 10.1007/s11249-010-9611-7

Rubinstein, S. M., Cohen, G., & Fineberg, J. (2007). Dynamics of precursors to frictional sliding. *Physical Review Letters*, *98*(22), 1–4. doi: 10.1103/PhysRevLett.98.226103